PHYSICAL REVIEW B VOLUME 47, NUMBER 2 1 JANUARY 1993-II

Magnetization of type-II superconductors in the Kim-Anderson model

K. Yamamoto
Ube Laboratory, Ube Industries Ltd. Ube 755, Japan

H. Mazaki and H. Yasuoka
Department of Mathematics and Physics, The National Defense Academy, Yokosuka 239, Japan
(Received 4 May 1992)

Within the construct of the complete Kim-Anderson model for the critical-current density, we have calculated the initial magnetization curves and full hysteresis loops of type-II superconductors immersed in an external field $H=H_{\rm dc}+H_{\rm ac}\cos(\omega t)$, where $H_{\rm dc}$ (≥ 0) is a dc bias field and $H_{\rm ac}$ (>0) is an ac field amplitude. We denote the maximum and minimum values of H by H_A ($=H_{\rm dc}+H_{\rm ac}$) and H_B ($=H_{\rm dc}-H_{\rm ac}$). According to the Kim-Anderson model, the critical-current density J_c is assumed to be a function of the local internal magnetic-flux density B_i, $J_c(B_i)=k/(B_0+|B_i|)$, where k and B_0 are constants. We consider an infinitely long cylinder with radius a, and the applied field along the cylinder axis. The field for full penetration is $H_p=[(B_0^2+2\mu_0ka)^{1/2}-B_0]/\mu_0$. A related parameter is $H^*=[(B_0^2-4\mu_0ka)^{1/2}-B_0]/\mu_0$. Magnetization equations for full hysteresis loops are derived for three different ranges of H_A: $0<H_A\leq H_p$, $H_p\leq H_A\leq H^*$, and $H^*\leq H_A$. Each of these three cases is further classified for several ranges of H_B. To describe completely the descending and ascending branches of the full hysteresis loops for all cases, 58 stages of H are considered and the appropriate magnetization equations are derived. In addition to these equations for a cylinder, the corresponding equations for a slab are presented. Comparison with previous work by Ji *et al.* and by Chen and Goldfarb in the appropriate limits supports the validity of the present derivation.

I. INTRODUCTION

The basic premise of the critical-state model introduced by Bean[1,2] and London[3] for the study of magnetic properties of type-II superconductors is that, when a magnetic field is applied to a sample, a macroscopic supercurrent circulates in the sample with a critical-current density $J_c(B_i)$, where B_i is the local flux density inside the specimen. An additional assumption for the critical-state model is that the lower critical field is zero.

Bean[2] derived the full hysteresis loop by assuming that J_c is a constant independent of B_i. On the assumption that the critical-current density as a function of B_i has the form

$$J_c=\frac{k}{B_0+|B_i|}\ , \tag{1}$$

where k and B_0 are constants, Kim, Hempstead, and Strnad[4,5] and Anderson[6] investigated the critical phenomena of type-II superconductors. As pointed out by Chen and Goldfarb,[7] the relation given by Eq. (1) is a very generalized form of the critical-state model because, when $B_0 \gg B_i$, it is equivalent to the linear model[8] $J_c(B_i)=A-C|B_i|$, where A and C are positive constants, and to the Bean model[2] when k and B_0 become infinite in such a way that k/B_0 is a constant. When $B_0=0$, it leads to the power-law model[9,10] $J_c(B_i)=k/|B_i|$, where the power of B_i is -1, the so-called simplified Kim model.

For every model mentioned above, one can derive the initial magnetization curve and hysteresis loops of superconductors. In the framework of the Kim-Anderson model,[4–6] Chen and Goldfarb[7] derived both the initial magnetization curve and the hysteresis loops for the case with no dc offset magnetic field. In the present study, we extend their derivation to the more generalized case where an alternating magnetic field is superimposed on a dc magnetic field, $H(\omega t)=H_{\rm dc}+H_{\rm ac}\cos(\omega t)$, where $H_{\rm dc}$ (≥ 0) is a dc basis field and $H_{\rm ac}$ (>0) is an ac field amplitude.

Using these extended equations, we calculate $M(H)$ curves and verify that the curves are continuous at their end points. For a further test of our derivations, we reduce the $M(H)$ equations in the limit $B_0 \to 0$ and compare them with the result by Ji *et al.*[11] who derived the magnetization equations in the framework of the simplified Kim model ($B_0=0$).

II. GENERAL EXPRESSIONS FOR MAGNETIZATION AND LOCAL CURRENT DENSITY FOR AN INFINITE CYLINDER

We consider an infinitely long cylindrical specimen with radius a, where the boundary of the sample is at $x=a$. An external field H is applied along the axis. In this configuration, both the local current density and the local magnetic-flux density are expressed as functions of x, and are denoted as $J(x)$ and $B_i(x)$, respectively.

In the critical-state model, by applying an external field H, macroscopic supercurrent $J(x)$ flows in the sample and $B_i(x)$ is written as

$$B_i(x)=\mu_0H+\mu_0\int_x^a J(x')dx'\ , \tag{2}$$

where $\mu_0=4\pi\times10^{-7}$ H/m. Using $B_i(x)$, we obtain the average flux density $B(H)$ in the sample

$$B(H)=\frac{2}{a^2}\int_0^a xB_i(x)dx \ . \tag{3}$$

Thus, the average magnetization $M(H)$ of the sample is given by

$$M(H)=B(H)/\mu_0-H \ . \tag{4}$$

Using the expression for critical current density $J_c=k/(B_0+|B_i|)$ and Ampere's law, $\nabla\times\mathbf{B}=\mu_0\mathbf{J}$, we obtain

$$\frac{dB_i}{dx}=-\mu_0 J(x)=\frac{-\mathrm{sgn}(J)\mu_0 k}{B_0+\mathrm{sgn}(B_i)B_i} \ , \tag{5}$$

where the sign function sgn(X) is 1 if $X>0$, -1 if $X<0$, and 0 if $X=0$. From Eq. (5),

$$\int [B_0+\mathrm{sgn}(B_i)B_i]dB_i=-\int \mathrm{sgn}(J)\mu_0 k\, dx \ . \tag{6}$$

After integration, we obtain

$$B_i=-\mathrm{sgn}(B_i)B_0\pm[B_0^2-\mathrm{sgn}(JB_i)2\mu_0 k(x+c)]^{1/2} \ , \tag{7}$$

where c is an integration constant to be determined by the boundary conditions. Multiplying Eq. (7) by sgn(B_i), we obtain

$$B_0+\mathrm{sgn}(B_i)B_i =\pm\mathrm{sgn}(B_i)[B_0^2-\mathrm{sgn}(JB_i)2\mu_0 k(x+c)]^{1/2} \ . \tag{8}$$

We set $\pm\mathrm{sgn}(B_i)=1$ because, from Eq. (1), the left-hand side of Eq. (8) is always positive. Using Eqs. (1) and (8), we obtain the general expression for $J(x)$:

$$J(x)=\mathrm{sgn}(J)J_c(B_i) =\frac{\mathrm{sgn}(J)k}{[B_0^2-\mathrm{sgn}(JB_i)2\mu_0 k(x+c)]^{1/2}} \ . \tag{9}$$

III. INITIAL MAGNETIZATION AND FULL-PENETRATION FIELD

A. Current distribution and full-penetration field H_p

We start from the initial state, $H=J(x)=B_i(x)=0$, and increase H in the direction of the cylinder axis. According to Lenz's law, the supercurrent J (of negative sign) begins to penetrate from the sample surface ($x=a$) inward. If the supercurrent penetrates until $x=x_0$, $J(x)$ is given from Eq. (9) as

$$J(x)=0 \quad (0\le x\le x_0) \ , \tag{10a}$$

$$J(x)=j_0(x)=\frac{-k}{[B_0^2+2\mu_0 k(x+c)]^{1/2}} \quad (x_0\le x\le a) \ , \tag{10b}$$

where $j_0(x)$ is defined as the supercurrent corresponding to $J(x)$ in the region $x_0\le x\le a$. From the boundary condition $j_0(a)=-J_c(\mu_0 H)$ we get

$$2\mu_0 kc=(B_0+\mu_0 H)^2-B_0^2-2\mu_0 ka \ . \tag{11}$$

Substituting Eq. (11) into Eq. (10b), we obtain

$$j_0(x)=\frac{-k}{[(B_0+\mu_0 H)^2-2\mu_0 k(a-x)]^{1/2}} =-k(p_0 x+q_0)^{-1/2} \ , \tag{12}$$

where

$$p_0=2\mu_0 k \ , \tag{12a}$$

$$q_0=(B_0+\mu_0 H)^2-2\mu_0 ka \ . \tag{12b}$$

From the boundary condition $j_0(x_0)=-J_c(0)$, x_0 can be obtained:

$$x_0=a-[(B_0+\mu_0 H)^2-B_0^2]/2\mu_0 k \ . \tag{13}$$

Since the full-penetration field H_p is H for $x_0=0$ [see Fig. 1(a) represented schematically by a straight-line segment], we obtain

$$H_p=[(B_0^2+2\mu_0 ka)^{1/2}-B_0]/\mu_0 \ . \tag{14}$$

B. Local flux density and $B(H)$

We consider the magnetization for two stages: $0<H\le H_p$ and $H_p\le H$.

For the first stage ($0<H\le H_p$), the distribution of flux density in the sample is

$$B_i(x)=0 \quad (0\le x\le x_0) \ , \tag{15a}$$

$$B_i(x)=b_0(x)=\mu_0 H+\mu_0\int_x^a j_0(x')dx' \quad (x_0\le x\le a) \ , \tag{15b}$$

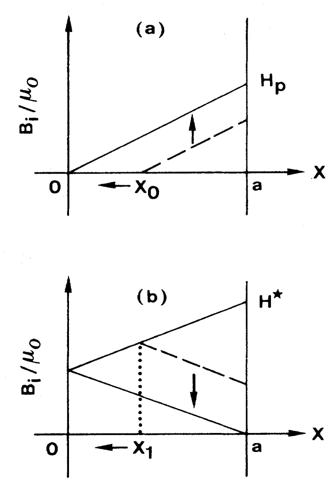

FIG. 1. Definition of (a) the full-penetration field H_p in the ascending branch and (b) a related parameter H^* in the descending branch, both represented schematically by straight-line segments. x_0 and x_1 are given by Eqs. (13) and (23), respectively, and a is the cylinder surface.

where $b_0(x)$ is defined by $B_i(x)$ derived using $j_0(x)$. Substituting Eq. (12) into Eq. (15b), we obtain

$$b_0(x)=(p_0x+q_0)^{1/2}-B_0 \ , \tag{16}$$

where we used $-2\mu_0k/p_0=-1$ and $(p_0a+q_0)^{1/2}=B_0+\mu_0H$.

Using Eq. (3), the average flux density for this case is

$$\begin{aligned}B(H)&=\frac{2}{a^2}\int_{x_0}^{a}xb_0(x)dx\\&=\frac{1}{15(\mu_0ka)^2}[(3p_0a-2q_0)(p_0a+q_0)^{3/2}\\&\qquad-(3p_0x_0-2q_0)(p_0x_0+q_0)^{3/2}]\\&\quad-(B_0/a^2)(a^2-x_0^2) \ .\end{aligned} \tag{17}$$

Similarly, in the following discussion, we use $j_m(x)$ ($m=0,1,2,\ldots,8$) which corresponds to $J(x)$ in a specified region of x for each m. Thus, we assign $b_m(x)$ to local flux density $B_i(x)$ derived by substituting $j_m(x)$ into Eq. (15b).

For simplicity, we define here $G_m(x)$ with p_m and q_m involved in $j_m(x)$:

$$G_m(x)=\frac{1}{15(\mu_0ka)^2}(3p_mx-2q_m)(p_mx+q_m)^{3/2} \ , \tag{18}$$

where

$$p_0=p_3=p_6=p_7=p_8=2\mu_0k \ , \tag{18a}$$

$$p_1=p_2=p_4=p_5=-2\mu_0k \ , \tag{18b}$$

$$q_0=q_6=q_7=q_8=(B_0+\mu_0H)^2-2\mu_0ka \ , \tag{18c}$$

$$q_1=(B_0+\mu_0H)^2+2\mu_0ka \ , \tag{18d}$$

$$q_2=2B_0^2-(B_0-\mu_0H)^2+2\mu_0ka \ , \tag{18e}$$

$$q_3=(B_0-\mu_0H)^2-2\mu_0ka \ , \tag{18f}$$

$$q_4=(B_0-\mu_0H)^2+2\mu_0ka \ , \tag{18g}$$

$$q_5=2B_0^2-(B_0+\mu_0H)^2+2\mu_0ka \ . \tag{18h}$$

Using $G_0(x)$ defined by Eq. (18), Eq. (17) can be rewritten as

$$B(H)=G_0(a)-G_0(x_0)-(B_0/a^2)(a^2-x_0^2) \ . \tag{19}$$

For the second stage ($H_p\le H$), $B(H)$ is given by Eq. (19) with $x_0=0$:

$$B(H)=G_0(a)-G_0(0)-B_0 \ . \tag{20}$$

IV. FULL HYSTERESIS LOOPS

To obtain full hysteresis loops, we consider a period of the applied field $H=H_{\rm dc}+H_{\rm ac}\cos(\omega t)$, where $H_{\rm dc}\ge 0$ and $H_{\rm ac}>0$. Denoting the maximum and minimum values of H by H_A ($=H_{\rm dc}+H_{\rm ac}$) and H_B ($=H_{\rm dc}-H_{\rm ac}$), respectively, three types of hysteresis loops appear, depending on the magnitude of H_A.

The first case is for $0<H_A\le H_p$, where the specimen is never fully penetrated. The second case is for $H^*\le H_A$, when the reverse supercurrent penetrates to the center of the specimen before H is cycled back to zero. [We give H^* schematically in Fig. 1(b), and its expression is derived below.] The third case is intermediate, $H_p\le H_A\le H^*$. When a dc bias field $H_{\rm dc}$ has a nonzero value, each of these cases is further classified into several different cases, depending on the magnitude of H_B.

A. Hysteresis loops for the low-H_A case ($0<H_A\le H_p$)

In the initial magnetization process, $B(H)$ for $H=H_A$ is obtained from Eq. (19):

$$B(H_A)=G_{0A}(a)-G_{0A}(x_{0A})-(B_0/a^2)(a^2-x_{0A}^2) \ , \tag{21}$$

where an additional subscript A on G_0 and x_0 indicates the specified function or variable at $H=H_A$. For example, from Eq. (13),

$$x_{0A}=a-[(B_0+\mu_0H_A)^2-B_0^2]/2\mu_0k) \ .$$

Full hysteresis loops are derived by decreasing H from H_A to H_B, forming the descending branch of the loops. The ascending branch is then drawn by increasing H from H_B to H_A.

1. For $H_B\le 0$

Stage 1: $0\le H\le H_A$ (descending). With decreasing H from H_A, the supercurrent J (of positive sign) penetrates from the sample surface until $x=x_1$, and the corresponding $j_1(x)$ is expressed by

$$j_1(x)=\frac{k}{[(B_0+\mu_0H)^2+2\mu_0k(a-x)]^{1/2}} \qquad (x_1\le x\le a) \ , \tag{22}$$

where we used the boundary condition $j_1(a)=J_c(\mu_0H)$. Using the boundary condition at $x=x_1$, $j_1(x_1)=-j_{0A}(x_1)$, we obtain

$$x_1=a-[(B_0+\mu_0H_A)^2-(B_0+\mu_0H)^2]/4\mu_0k \ . \tag{23}$$

Thus, the corresponding flux density $b_1(x)$ in the region $x_1\le x\le a$ and $B(H)$ is

$$b_1(x)=(p_1x+q_1)^{1/2}-B_0 \ , \tag{24}$$

$$\begin{aligned}B(H)&=\frac{2}{a^2}\left[\int_{x_{0A}}^{x_1}xb_{0A}(x)dx+\int_{x_1}^{a}xb_1(x)dx\right]\\&=[G_1(a)-G_1(x_1)]+[G_{0A}(x_1)-G_{0A}(x_{0A})]\\&\quad-(B_0/a^2)(a^2-x_{0A}^2) \ .\end{aligned} \tag{25}$$

Stage 2: $H_B\le H\le 0$ (descending). For $H=0$, $j_1(x)$ takes its maximum value at $x=a$, $j_1(a)=k/B_0$. With decreasing H, x at which the supercurrent becomes maximum [i.e., equivalent to $B_i(x)=0$] shifts inward until $x=x_3$. In this case, the supercurrent, denoted by $j_3(x)$, is

$$j_3(x)=\frac{k}{[(B_0-\mu_0H)^2-2\mu_0k(a-x)]^{1/2}} \quad (x_3\le x\le a)\ , \tag{26}$$

where we used the boundary condition $j_3(a)=J_c(\mu_0H)$. From the boundary condition $j_3(x_3)=J_c(0)$, we find

$$x_3=a-[(B_0-\mu_0H)^2-B_0^2]/2\mu_0k\ . \tag{27}$$

Assigning x_2 to the point $x=x_1$ at which the supercurrent turns around, and expressing $J(x)$ in the region $x_2\le x\le x_3$ by $j_2(x)$, we obtain

$$j_2(x)=\frac{k}{[(2B_0^2-(B_0-\mu_0H)^2+2\mu_0k(a-x)]^{1/2}} \quad (x_2\le x\le x_3)\ , \tag{28}$$

where we used $j_2(x_3)=j_3(x_3)$. From the boundary condition $j_2(x_2)=-j_{0A}(x_2)$, x_2 is given by

$$x_2=a-[(B_0+\mu_0H_A)^2+(B_0-\mu_0H)^2-2B_0^2]/4\mu_0k\ . \tag{29}$$

Thus, we obtain $b_2(x)$, $b_3(x)$, and $B(H)$:

$$b_2(x)=(p_2x+q_2)^{1/2}-B_0\ , \tag{30}$$

$$b_3(x)=-(p_3x+q_3)^{1/2}+B_0\ , \tag{31}$$

$$\begin{aligned}B(H)=&-[G_3(a)-G_3(x_3)]+[G_2(x_3)-G_2(x_2)]\\&+[G_{0A}(x_2)-G_{0A}(x_{0A})]\\&+(B_0/a^2)(a^2+x_{0A}^2-2x_3^2)\ .\end{aligned} \tag{32}$$

Stage 3: $H_B\le H\le 0$ (ascending). When H increases from H_B, the supercurrent (of negative sign) circulates in the sample. Supposing the supercurrent penetrates until $x=x_4$, and assigning $j_4(x)$ to $J(x)$ in the region $x_4\le x\le a$, we obtain the following equations in a similar way as discussed above:

$$j_4(x)=\frac{-k}{[(B_0-\mu_0H)^2+2\mu_0k(a-x)]^{1/2}} \quad (x_4\le x\le a)\ , \tag{33}$$

$$x_4=a-[(B_0-\mu_0H_B)^2-(B_0-\mu_0H)^2]/4\mu_0k\ , \tag{34}$$

$$b_4(x)=-(p_4x+q_4)^{1/2}+B_0\ , \tag{35}$$

$$\begin{aligned}B(H)=&-[G_4(a)-G_4(x_4)]-[G_{3B}(x_4)-G_{3B}(x_{3B})]\\&+[G_{2B}(x_{3B})-G_{2B}(x_{2B})]\\&+[G_{0A}(x_{2B})-G_{0A}(x_{0A})]\\&+(B_0/a^2)(a^2+x_{0A}^2-2x_{3B}^2)\ ,\end{aligned} \tag{36}$$

where an additional subscript B on G and x indicates the specified function or variable at $H=H_B$.

Stage 4: $0\le H\le H_C$ (ascending). For $H=0$, $j_4(x)$ has its minimum value at $x=a$, $j_4(a)=-k/B_0$. With increasing H, x at which the supercurrent becomes minimum [i.e., equivalent to $B_i(x)=0$] shifts inward until $x=x_6$. We assign $j_6(x)$ to $J(x)$ in the region $x_6\le x\le a$. We also assign x_5 ($<x_6$) to the point at which $J(x)$ turns around from negative to positive, and in the region $x_5\le x\le x_6$, we use $j_5(x)$. H_C is defined as H for $x_5=x_{3B}$. Since H_C is positive, we find $H_C=-H_B$. Thus, by a similar method, we obtain

$$j_5(x)=\frac{-k}{[2B_0^2-(B_0+\mu_0H)^2+2\mu_0k(a-x)]^{1/2}} \quad (x_5\le x\le x_6)\ , \tag{37}$$

$$x_5=a-[(B_0+\mu_0H)^2+(B_0-\mu_0H_B)^2-2B_0^2]/4\mu_0k\ , \tag{38}$$

$$b_5(x)=-(p_5x+q_5)^{1/2}+B_0\ , \tag{39}$$

$$j_6(x)=\frac{-k}{[(B_0+\mu_0H)^2-2\mu_0k(a-x)]^{1/2}} \quad (x_6\le x\le a)\ , \tag{40}$$

$$x_6=a-[(B_0+\mu_0H)^2-B_0^2]/2\mu_0k\ , \tag{41}$$

$$b_6(x)=(p_6x+q_6)^{1/2}-B_0\ , \tag{42}$$

$$\begin{aligned}B(H)=&[G_6(a)-G_6(x_6)]-[G_5(x_6)-G_5(x_5)]-[G_{3B}(x_5)-G_{3B}(x_{3B})]+[G_{2B}(x_{3B})-G_{2B}(x_{2B})]\\&+[G_{0A}(x_{2B})-G_{0A}(x_{0A})]-(B_0/a^2)[a^2-x_{0A}^2+2(x_{3B}^2-x_6^2)]\ .\end{aligned} \tag{43}$$

Note that $j_6(x)=j_0(x)$, $b_6(x)=b_0(x)$, $x_6=x_0$, and $G_6(x)=G_0(x)$.

Stage 5: $-H_B\le H\le H_A$ (ascending). Considering that the supercurrent changes its sign from negative to positive at a certain point, denoted by x_7, we define $J(x)$ in the region $x_7\le x\le a$ as $j_7(x)$:

$$j_7(x)=\frac{-k}{[(B_0+\mu_0H)^2-2\mu_0k(a-x)]^{1/2}} \quad (x_7\le x\le a)\ , \tag{44}$$

$$x_7=a-[(B_0+\mu_0H)^2+(B_0-\mu_0H_B)^2-2B_0^2]/4\mu_0k\ , \tag{45}$$

$$b_7(x)=(p_7x+q_7)^{1/2}-B_0 , \quad (46)$$

$$B(H)=[G_7(a)-G_7(x_7)]+[G_{2B}(x_7)-G_{2B}(x_{2B})] +[G_{0A}(x_{2B})-G_{0A}(x_{0A})] +(B_0/a^2)(a^2-x_{0A}^2) . \quad (47)$$

Note that $j_7(x)=j_0(x)$, $b_7(x)=b_0(x)$, $x_7=x_5$, and $G_7(x)=G_0(x)$.

2. For $H_B \geq 0$

Stage 1: $H_B \leq H \leq H_A$ (descending). This stage is the same as stage 1 of Sec. IV A 1 except for the interval of H. $B(H)$ is given by Eq. (25).

Stage 2: $H_B \leq H \leq H_A$ (ascending). Supposing that the supercurrent penetrates until $x=x_8$ with the increase of H, and assigning $j_8(x)$ to $J(x)$ in the region $x_8 \leq x \leq a$, we obtain

$$j_8(x)=\frac{-k}{[(B_0+\mu_0H)^2-2\mu_0k(a-x)]^{1/2}} \quad (x_8 \leq x \leq a) , \quad (48)$$

$$x_8=a-[(B_0+\mu_0H)^2-(B_0-\mu_0H_B)^2]/4\mu_0k , \quad (49)$$

$$b_8(x)=(p_8x+q_8)^{1/2}-B_0 , \quad (50)$$

$$B(H)=[G_8(a)-G_8(x_8)]+[G_{1B}(x_8)-G_{1B}(x_{1B})] +[G_{0A}(x_{1B})-G_{0A}(x_{0A})] -(B_0/a^2)(a^2-x_{0A}^2) . \quad (51)$$

Note that $j_8(x)=j_0(x)$, $b_8(x)=b_0(x)$, and $G_8(x)=G_0(x)$.

B. Hysteresis loops for the medium-H_A case ($H_p \leq H_A \leq H^*$)

In the intermediate case, there are four cases depending on the magnitude of H_B. To avoid repetition, we give only the final $B(H)$ equations derived by a similar process as described above.

1. For $H_B \leq -H_p$

Stage 1: $0 \leq H \leq H_A$ (descending):

$$B(H)=[G_1(a)-G_1(x_1)] +[G_{0A}(x_1)-G_{0A}(0)]-B_0 . \quad (52)$$

This equation is the same as Eq. (25) with $x_{0A}=0$. Since $x_1=0$ for $H=0$, H^* is expressed as

$$H^*=[(B_0^2+4\mu_0ka)^{1/2}-B_0]/\mu_0 . \quad (53)$$

Stage 2: $H_{prm}^- \leq H \leq 0$ (descending). H_{prm}^- is the reverse full-penetration field (on the descending branch) for the medium-H_A case, which is represented schematically in Fig. 2(a). H_{prm}^- can be determined by taking $x_2=0$ in Eq. (29):

$$H_{prm}^-=B_0/\mu_0 -[4\mu_0ka+2B_0^2-(B_0+\mu_0H_A)^2]^{1/2}/\mu_0 , \quad (54)$$

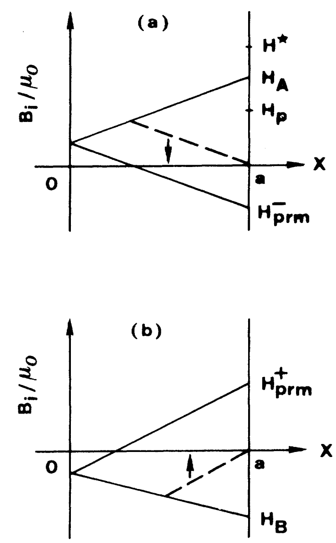

FIG. 2. Schematic representations of the reverse full-penetration fields (a) H_{prm}^- in the descending branch and (b) H_{prm}^+ in the ascending branch for the medium-H_A case. H_A and H_B are the maximum and minimum values of H, respectively.

$$B(H)=-[G_3(a)-G_3(x_3)]+[G_2(x_3)-G_2(x_2)] +[G_{0A}(x_2)-G_{0A}(0)] -(B_0/a^2)(a^2-2x_3^2) . \quad (55)$$

Stage 3: $-H_p \leq H \leq H_{prm}^-$ (descending):

$$B(H)=-[G_3(a)-G_3(x_3)]+[G_2(x_3)-G_2(0)] +(B_0/a^2)(a^2-2x_3^2) . \quad (56)$$

Stage 4: $H_B \leq H \leq -H_p$ (descending):

$$B(H)=-[G_3(a)-G_3(0)]+B_0 . \quad (57)$$

Stage 5: $H_B \leq H \leq 0$ (ascending):

$$B(H)=-[G_4(a)-G_4(x_4)] -[G_{3B}(x_4)-G_{3B}(0)]+B_0 . \quad (58)$$

Stage 6: $0 \leq H \leq H_{prm}^+$ (ascending). H_{prm}^+ is the reverse full-penetration field (on the ascending branch) for the medium-H_A case which is represented schematically in Fig. 2(b). H_{prm}^+ can be determined by taking $x_5=0$ in Eq. (38):

$$H_{prm}^+=[4\mu_0ka+2B_0^2-(B_0-\mu_0H_B)^2]^{1/2}/\mu_0-B_0/\mu_0 , \quad (59)$$

$$B(H)=[G_6(a)-G_6(x_6)]-[G_5(x_6)-G_5(x_5)] -[G_{3B}(x_5)-G_{3B}(0)]-(B_0/a^2)(a^2-2x_6^2) . \quad (60)$$

Stage 7: $H_{prm}^+ \leq H \leq H_p$ (ascending):

$$B(H)=[G_6(a)-G_6(x_6)]-[G_5(x_6)-G_5(0)] -(B_0/a^2)(a^2-2x_6^2) . \quad (61)$$

Stage 8: $H_p \le H \le H_A$ (ascending):

$$B(H)=[G_6(a)-G_6(0)]-B_0 \ . \tag{62}$$

2. For $-H_p \le H_B \le H_{prm}^-$

Stage 1: $0 \le H \le H_A$ (descending). Same as Eq. (52).

Stage 2: $H_{prm}^- \le H \le 0$ (descending). Same as Eq. (55).

Stage 3: $H_B \le H \le H_{prm}^-$ (descending). This stage is the same as stage 3 of Sec. IV B 1 except for the interval of H. $B(H)$ is given by Eq. (56).

Stage 4: $H_B \le H \le 0$ (ascending):

$$B(H)=-[G_4(a)-G_4(x_4)]-[G_{3B}(x_4)-G_{3B}(x_{3B})] +[G_{2B}(x_{3B})-G_{2B}(0)]-(B_0/a^2)(a^2-2x_3^2) \ . \tag{63}$$

Stage 5: $0 \le H \le -H_B$ (ascending):

$$B(H)=[G_6(a)-G_6(x_6)]-[G_5(x_6)-G_5(x_5)] -[G_{3B}(x_5)-G_{3B}(x_{3B})]+[G_{2B}(x_{3B})-G_{2B}(0)] -(B_0/a^2)(a^2+2x_{3B}^2-2x_6^2) \ . \tag{64}$$

Stage 6: $-H_B \le H \le H_{prm}^+$ (ascending):

$$B(H)=[G_7(a)-G_7(x_7)] +[G_{2B}(x_7)-G_{2B}(0)]-B_0 \ . \tag{65}$$

Stage 7: $H_{prm}^+ \le H \le H_A$ (ascending). Same as Eq. (62).

3. For $H_{prm}^- \le H_B \le 0$

Stage 1: $0 \le H \le H_A$ (descending). Same as in Eq. (52).

Stage 2: $H_B \le H \le 0$ (descending). This stage is the same as stage 2 of Sec. IV B 1 except for the interval of H. $B(H)$ is given by Eq. (55).

Stage 3: $H_B \le H \le 0$ (ascending):

$$B(H)=-[G_4(a)-G_4(x_4)]-[G_{3B}(x_4)-G_{3B}(x_{3B})] +[G_{2B}(x_{3B})-G_{2B}(x_{2B})] +[G_{0A}(x_{2B})-G_{0A}(0)]+(B_0/a^2)(a^2-2x_3^2) \ . \tag{66}$$

Stage 4: $0 \le H \le -H_B$ (ascending):

$$B(H)=[G_6(a)-G_6(x_6)]-[G_5(x_6)-G_5(x_5)]-[G_{3B}(x_5)-G_{3B}(x_{3B})]+[G_{2B}(x_{3B})-G_{2B}(x_{2B})] +[G_{0A}(x_{2B})-G_{0A}(0)]-(B_0/a^2)(a^2+2x_{3B}^2-2x_6^2) \ . \tag{67}$$

Stage 5: $-H_B \le H \le H_A$ (ascending):

$$B(H)=[G_7(a)-G_7(x_7)]+[G_{2B}(x_7)-G_{2B}(x_{2B})] +[G_{0A}(x_{2B})-G_{0A}(0)]-B_0 \ . \tag{68}$$

4. For $0 \le H_B < H_A$

Stage 1: $H_B \le H \le H_A$ (descending). This stage is the same as stage 1 of Sec. IV B 1 except for the interval of H. $B(H)$ is given by Eq. (52).

Stage 2: $H_B \le H \le H_A$ (ascending):

$$B(H)=[G_8(a)-G_8(x_8)]+[G_{1B}(x_8)-G_{1B}(x_{1B})] +[G_{0A}(x_{1B})-G_{0A}(0)]-B_0 \ . \tag{69}$$

C. Hysteresis loops for the high-H_A case ($H^* \le H_A$)

1. For $H_B \le -H^*$

Stage 1: $H_{prh}^- \le H \le H_A$ (descending). H_{prh}^- is the reverse full-penetration field (on the descending branch) for the high-H_A case, which is represented schematically in Fig. 3(a). H_{prh}^- can be determined by taking $x_1=0$ in Eq. (23):

$$H_{prh}^- = [(B_0+\mu_0 H_A)^2-4\mu_0 ka]^{1/2}/\mu_0 - B_0/\mu_0 \ , \tag{70}$$

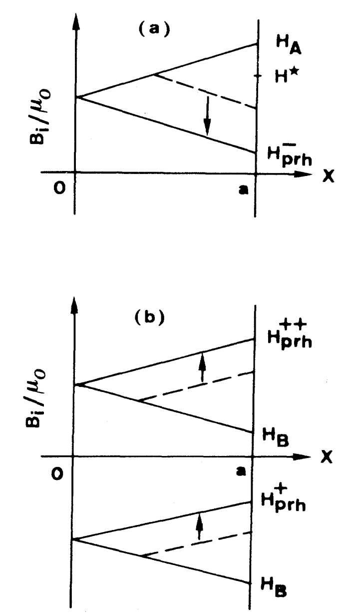

FIG. 3. Schematic representations of the reverse full-penetration fields (a) H_{prh}^- in the descending branch, H_{prh}^+ in the ascending branch, and H_{prh}^{++} in the ascending branch. When $H=H_{prh}^-$, H_{prh}^+, or H_{prh}^{++}, $B_i(x)$ never crosses over the x axis.

$$B(H)=[G_1(a)-G_1(x_1)]+[G_{0A}(x_1)-G_{0A}(0)]-B_0 . \quad (71)$$

Stage 2: $0 \le H \le H_{prh}^-$ (descending):

$$B(H)=[G_1(a)-G_1(0)]-B_0 . \quad (72)$$

Stage 3: $-H_p \le H \le 0$ (descending). This stage is the same as stage 3 of Sec. IV B 1 except for the interval of H. $B(H)$ is given by Eq. (56).

Stage 4: $H_B \le H \le -H_p$ (descending). Same as Eq. (57).

Stage 5: $H_B \le H \le H_{prh}^+$ (ascending). H_{prh}^+ is the reverse full-penetration field (on the ascending branch) for the high-H_A case, which is represented schematically in Fig. 3(b). H_{prh}^+ can be determined by taking $x_4=0$ in Eq. (34):

$$H_{prh}^+=B_0/\mu_0-[(B_0-\mu_0 H_B)^2-4\mu_0 ka]^{1/2}/\mu_0 . \quad (73)$$

This stage is the same as stage 5 of Sec. IV B 1 except for the interval of H. $B(H)$ is given by Eq. (58).

Stage 6: $H_{prh}^+ \le H \le 0$ (ascending):

$$B(H)=-[G_4(a)-G_4(0)]+B_0 . \quad (74)$$

Stage 7: $0 \le H \le H_p$ (ascending). This stage is the same as stage 7 of Sec. IV B 1 except for the interval of H. $B(H)$ is given by Eq. (61).

Stage 8: $H_p \le H \le H_A$ (ascending). Same as Eq. (62).

2. For $-H^* \le H_B \le -H_p$

Stage 1: $H_{prh}^- \le H \le H_A$ (descending). Same as Eq. (71).

Stage 2: $0 \le H \le H_{prh}^-$ (descending). Same as Eq. (72).

Stage 3: $-H_p \le H \le 0$ (descending). This stage is the same as stage 3 of Sec. IV B 1 except for the interval of H. $B(H)$ is given by Eq. (56).

Stage 4: $H_B \le H \le -H_p$ (descending). Same as Eq. (57).

Stage 5: $H_B \le H \le 0$ (ascending). Same as Eq. (58).

Stage 6: $0 \le H \le H_{prm}^+$ (ascending). Same as Eq. (60).

Stage 7: $H_{prm}^+ \le H \le H_p$ (ascending). Same as Eq. (61).

Stage 8: $H_p \le H \le H_A$ (ascending). Same as Eq. (62).

3. For $-H_p \le H_B \le 0$

Stage 1: $H_{prh}^- \le H \le H_A$ (descending). Same as Eq. (71).

Stage 2: $0 \le H \le H_{prh}^-$ (descending). Same as Eq. (72).

Stage 3: $H_B \le H \le 0$ (descending). This stage is the same as stage 3 of Sec. IV B1 except for the interval of H. $B(H)$ is given by Eq. (56).

Stage 4: $H_B \le H \le 0$ (ascending). Same as Eq. (63).

Stage 5: $0 \le H \le -H_B$ (ascending). Same as Eq. (64).

Stage 6: $-H_B \le H \le H_{prm}^+$ (ascending). Same as Eq. (65).

Stage 7: $H_{prm}^+ \le H \le H_A$ (ascending). This stage is the same as stage 8 of Sec. IV B 1 except for the interval of H. $B(H)$ is given by Eq. (62).

4. For $0 \le H_B \le H_{prh}^-$

Stage 1: $H_{prh}^- \le H \le H_A$ (descending). Same as Eq. (71).

Stage 2: $H_B \le H \le H_{prh}^-$ (descending). This stage is the same as stage 2 of Sec. IV C1 except for the interval of H. $B(H)$ is given by Eq. (72).

Stage 3: $H_B \le H \le H_{prh}^{++}$ (ascending). H_{prh}^{++} is the reverse full-penetration field (on the ascending branch) for the high-H_A case, which is represented schematically in Fig. 3(b). H_{prh}^{++} can be determined by taking $x_8=0$ in Eq. (49):

$$H_{prh}^{++}=[(B_0+\mu_0 H_B)^2+4\mu_0 ka]^{1/2}/\mu_0-B_0/\mu_0 , \quad (75)$$

$$B(H)=[G_8(a)-G_8(x_8)]+[G_{1B}(x_8)-G_{1B}(0)]-B_0 . \quad (76)$$

Stage 4: $H_{prh}^{++} \le H \le H_A$ (ascending). This stage is the same as stage 8 of Sec. IV B 1 except for the interval of H. $B(H)$ is given by Eq. (62).

5. For $H_{prh}^- \le H_B < H_A$

Stage 1: $H_B \le H \le H_A$ (descending). This stage is the same as stage 1 of Sec. IV C 1 except for the interval of H. $B(H)$ is given by Eq. (71).

Stage 2: $H_B \le H \le H_A$ (ascending). Same as Eq. (69).

V. COMPUTED $M(H)$ CURVES

We have analytically tested, for each case in Sec. IV, that the stages are continuous at their end points. In this section, we give some computed $M(H)$ curves. To reduce the number of variables, we define a parameter, similar to one used by Kim[5] and Chen and Goldfarb:[7]

$$p=(2\mu_0 ka)^{1/2}/B_0 . \quad (77)$$

Using this parameter p, Eqs. (14) and (53) can be rewritten as

$$H_p=B_0[(1+p^2)^{1/2}-1]/\mu_0 , \quad (78)$$

$$H^*=B_0[(1+2p^2)^{1/2}-1]/\mu_0 . \quad (79)$$

$M(H)$ is calculated from $B(H)$ using Eq. (4). Figures 4–6 give the initial and hysteresis $M(H)$ curves for three different values of dc bias field, $H_{dc}=0$, H_p, and $4H_p$; and for each H_{dc}, three different values of p: 0.3, 3, and 1000. For each case, three $M(H)$ loops are drawn for $H_{ac}=H_p/2$, $(H^*+H_p)/2$, and $4H_p$. For all the loops, M and H are normalized to H_p. Figures 4(a)–4(c) correspond to Figs. 6(a), 6(c), and 6(e) in Ref. 7, in which the physical interpretation of the $M(H)$ behavior has been thoroughly discussed.

From Figs. 4–6, we note the following aspects.

(a) As seen in Fig. 4 ($H_{dc}=0$), the $M(H)$ loops are symmetrical about the origin of the coordinate axes. Figure 4(a) is very similar to those derived from Bean's model;[2] in the limit $p \to 0$, the $M(H)$ loops exactly reduce to those from Bean's model.

(b) When $H_{dc}>0$, the center of the $M(H)$ loops shifts

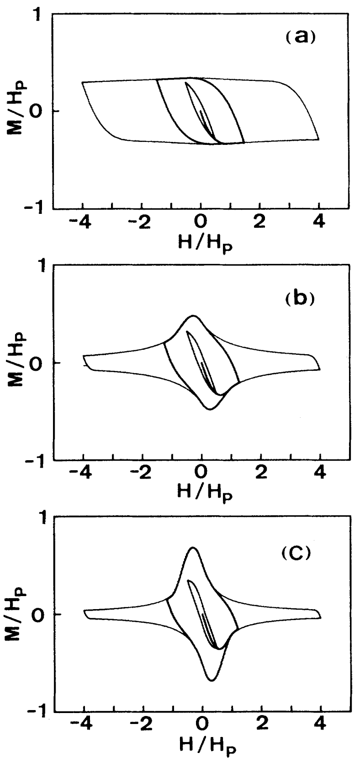

FIG. 4. Theoretical M-H curves, scales by H_p, for $H_{\mathrm{dc}}=0$ and $p=$(a) 0.3, (b) 3, and (c) 1000. In each figure, loops are shown for $H_{\mathrm{ac}}=H_p/2$ (smallest), $(H^*+H_p)/2$, and $4H_p$ (largest).

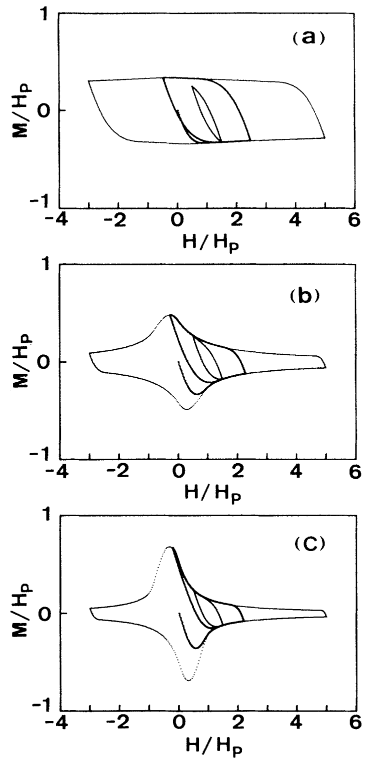

FIG. 5. Theoretical M-H curves, scaled by H_p, for $H_{\mathrm{dc}}=H_p$ and $p=$(a) 0.3, (b) 3, and (c) 1000. In each figure, loops are shown for $H_{\mathrm{ac}}=H_p/2$ (smallest), $(H^*+H_p)/2$, and $4H_p$ (largest).

to the right (by $H/H_p=1$ in Fig. 5 and by $H/H_p=4$ in Fig. 6), and the profiles of the $M(H)$ curves become more and more asymmetrical about the center as p increases.

(c) The asymmetrical nature is more evident for $H_{\mathrm{dc}}\approx H_{\mathrm{ac}}$. This can be seen, for example, by comparing the outermost loop in Fig. 6(c) ($H_{\mathrm{dc}}=4H_p$, $H_{\mathrm{ac}}=4H_p$) with the innermost loop in the same figure ($H_{\mathrm{dc}}=4H_p$, $H_{\mathrm{ac}}=H_p/2$).

(d) For $H_{\mathrm{dc}}\gg H_{\mathrm{ac}}$, the asymmetrical nature is much reduced and the $M(H)$ loops seem to approach those from Bean's model. [See, for example, the innermost loop in Fig. 6(c), where $H_{\mathrm{dc}}=4H_p$ and $H_{\mathrm{ac}}=H_p/2$.] The reason is that the effect of the variation of B_i on $J_c=k/(B_0+|B_i|)$ becomes relatively small.

VI. $B(H)$ EQUATIONS CORRESPONDING TO AN INFINITE SLAB

We modify our derivation to apply it to an infinitely long slab of thickness D. In this case, the local magnetic-flux density $B_i(x)$ and the average flux density given by Eqs. (2) and (3) are revised as

$$B_i(x)=\mu_0 H+\mu_0\int_x^{D/2} J(x')dx' , \tag{80}$$

$$B(H)=\frac{2}{D}\int_0^{D/2} B_i(x)dx . \tag{81}$$

The analytical forms of $M(H)$ and $J(x)$ given by Eqs. (4) and (9) hold in this case. From the boundary condition $j_0(D/2)=-J_c(\mu_0 H)$, Eq. (11) is revised as

$$2\mu_0 kc=(B_0+\mu_0 H)^2-B_0^2-2\mu_0 k(D/2) . \tag{82}$$

Substituting Eq. (82) into Eq. (10b), we obtain

$$j_0(x)=\frac{-k}{[(B_0+\mu_0 H)^2-\mu_0 k(D-2x)]^{1/2}}$$
$$=-k(p_0 x+q_0)^{-1/2} , \tag{83}$$

where $p_0=2\mu_0 k$ and $q_0=(B_0+\mu_0 H)^2-\mu_0 kD$. From the boundary condition $j_0(x_0)=-J_c(0)$, x_0 for the slab is

$$x_0=\frac{D}{2}-[(B_0+\mu_0 H)^2-B_0]/2\mu_0 k . \tag{84}$$

Since the full-penetration field H_p is the field for $x_0=0$, we obtain

$$H_p=[(B_0^2+\mu_0 kD)^{1/2}-B_0]/\mu_0 . \tag{85}$$

Referring to Eq. (15), and using Eqs. (81) and (83), the average flux density $B(H)$ in the slab is

$$B(H)=\frac{2}{D}\int_{x_0}^{D/2} b_0(x)dx$$
$$=\frac{2}{D}\int_{x_0}^{D/2}[(p_0x+q_0)^{1/2}-B_0]dx$$
$$=\frac{4}{3p_0D}[(p_0D/2+q_0)^{3/2}-(p_0x_0+q_0)^{3/2}]$$
$$-(2B_0/D)(D/2-x_0)\ .$$

Similar to $G_m(x)$ defined by Eq. (18), we here introduce a function $F_m(x)$ defined by

$$F_m(x)=\frac{4}{3p_mD}(p_mx+q_m)^{3/2}\quad (m=0,1,2,\ldots,8)\ , \tag{87}$$

where p_m and q_m are given by Eqs. (18a)–(18h). Note that, for the slab sample, a included in q_m should be replaced by $D/2$.

Using $F_m(x)$, Eq. (86) can be rewritten as

$$B(H)=F_0(D/2)-F_0(x_0)-(2B_0/D)(D/2-x_0)\ . \tag{88}$$

In a similar manner, we can derive all the $B(H)$ equations for a slab sample of thickness D from those for a cylinder sample of radius a. Analytically, this can be achieved as follows: (a) Replace a included in the $B(H)$ equations for a cylinder sample by $D/2$ except for the last term; for example, $(B_0/a^2)(a^2-x_0^2)$ in Eq. (19). In the last term, a^2 and x_m^2 should be replaced by D and $2x_m$, respectively. (b) Replace $G_m(x)$ by $F_m(x)$.

As an example, we derive $B(H)$ for a slab sample of thickness D for the high-H_A case, Sec. IV C1, stage 1, where $H_B \le -H^*$ and $H_{prh}^- \le H \le H_A$ (descending). Replacing $G_m(x)$ in Eq. (71) by $F_m(x)$, we obtain

$$B(H)=[F_1(D/2)-F_1(x_1)]$$
$$+[F_{0A}(x_1)-F_{0A}(0)]-B_0\ , \tag{89}$$

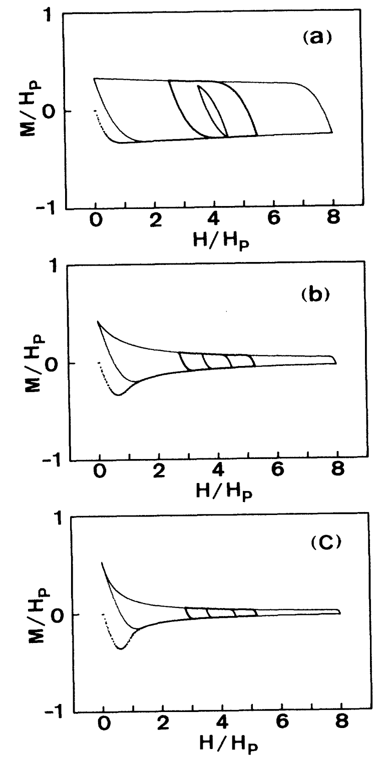

FIG. 6. Theoretical M-H curves, scaled by H_p, for $H_{\rm dc}=4H_p$ and $p=$(a) 0.3, (b) 3, and (c) 1000. In each figure, loops are shown for $H_{\rm ac}=H_p/2$ (smallest), $(H^*+H_p)/2$, and $4H_p$ (largest).

where an additional subscript A on F_0 indicates the specified F_0 at $H=H_A$.

Using Eq. (87) for $m=0$ and 1, and Eqs. (18a)–(18d), we obtain $B(H)$ for the case $B_0=0$:

$$B(H)=\frac{4}{3(-2\mu_0k)D}\{(\mu_0H)^3-[(-2\mu_0kx_1)+(\mu_0H)^2+\mu_0kD]^{3/2}$$
$$-[2\mu_0kx_1+(\mu_0H_A)^2-\mu_0kD]^{3/2}+[(\mu_0H_A)^2-\mu_0kD]^{3/2}\}\ . \tag{90}$$

Substituting

$$x_1=(D/2)-[(\mu_0H_A)^2-(\mu_0H)^2]/4\mu_0k$$

given by Eq. (23) into Eq. (90), we obtain

$$B(H)=\frac{-2}{3\mu_0kD}\{(\mu_0H)^3-[(\mu_0H_A)^2/2+(\mu_0H)^2/2]^{3/2}$$
$$-[(\mu_0H_A)^2/2+(\mu_0H)^2/2]^{3/2}$$
$$+[(\mu_0H_A)^2-\mu_0kD]^{3/2}\}\ . \tag{91}$$

From Eq. (14), $\mu_0kD=(\mu_0H_p)^2$. Using this relation, $B(H)$ is finally written as

$$B(H)=\frac{2}{3(\mu_0H_p)^2}\{2[(\mu_0H_A)^2/2+(\mu_0H)^2/2]^{3/2}-(\mu_0H)^3$$
$$-[(\mu_0H_A)^2-(\mu_0H_p)^2]^{3/2}\}\ . \tag{92}$$

There are several studies treating magnetization of a slab sample immersed in an ac field superimposed on a dc bias field. Employing the Kim-Anderson model,[4–6] Müller[12] calculated the fundamental ac susceptibility of a ceramic Y-Ba-Cu-O superconductor and compared with the experimental data of Goldfarb *et al.*,[13] even though

Müller did not give $M(H)$ equations used in the calculation.

Using the simplified Kim model[9,10] ($B_0=0$), Ji *et al.*[11] derived $B(H)$ equations for an infinitely long slab of thickness D, where the boundary of the sample is at $x=D/2$. The sample is immersed in a field H cycled between H_A and H_B, where $H_A>H_B$.

We find that Eq. (92) agrees with the first Eq. (14) of Ref. 11. From Eq. (70), the lower limit of H, H_{prh}^-, for $B_0=0$ is

$$H_{prh}^- = [(\mu_0 H_A)^2 - 2(\mu_0 kD)]^{1/2}/\mu_0 = [(\mu_0 H_A)^2 - 2(\mu_0 H_p)^2]^{1/2}/\mu_0 \; . \tag{93}$$

H_{prh}^- also agrees with the expression given by them.

In order to complete the descending branch for the high-H_A case, Sec. IV C1, for a slab sample, we also revised $B(H)$ of stages 2–4, Eqs. (72), (56), and (57), respectively. The results are the following.

Stage 2:

$$B(H) = \frac{2}{3(\mu_0 H_p)^2}\{[(\mu_0 H)^2 + (\mu_0 H_p)^2]^{3/2} - (\mu_0 H)^3\} \; . \tag{94}$$

Stage 3:

$$B(H) = \frac{2}{3(\mu_0 H_p)^2}\{[-(\mu_0 H)^2 + (\mu_0 H_p)^2]^{3/2} - (\mu_0 H)^3\} \; . \tag{95}$$

Stage 4:

$$B(H) = \frac{2}{3(\mu_0 H_p)^2}\{[(\mu_0 H)^2 - (\mu_0 H_p)^2]^{3/2} - (\mu_0 H)^3\} \; . \tag{96}$$

These equations agree with the second Eq. (14) in Ref. 11. The agreement in $B(H)$ equations supports the validity of our results.

VII. CONCLUSIONS

In the framework of the Kim-Anderson model[4–6] for critical-current density, Eq. (1), we have analytically derived magnetization equations for type-II superconductors immersed in an external magnetic field. We considered an infinitely long cylindrical specimen with the external field applied along the cylinder axis, and an infinite slab with the field in the plane. To obtain full hysteresis loops, we treated a period of the applied field $H=H_{dc}+H_{ac}\cos(\omega t)$, where $H_{dc}\geq 0$ and $H_{ac}>0$. Denoting the maximum and minimum values of H by H_A and H_B, respectively, three types of hysteresis loops appear, depending on the magnitude of H_A. Each of these three cases is further classified into several cases, depending on the magnitude of H_B. Full hysteresis loops were derived by decreasing H from H_A to H_B, forming the descending branch of the loop. The ascending branch was then formed by increasing H from H_B to H_A. To complete the descending and ascending branches for all the cases, we calculated 58 stages for H and all the magnetization equations were derived.

To test our derivation, we gave some computed magnetization curves with no dc offset magnetic field and compared them with those computed by Chen and Goldfarb.[7] For further examination of our results, our slab equations were tested in the limit $B_0\rightarrow 0$ in Eq. (1). We found the results agree with those by Ji *et al.*[11] who derived magnetization equations for the simplified Kim model.[9,10]

Recently, Ishida and Goldfarb[14] carried out detailed measurements and analyses of harmonic susceptibilities for a sintered Y-Ba-Cu-O superconductor where they superimposed a dc field on an ac field. They analyzed the results with the simplified Kim model and found that the temperature- and field-dependent features of the susceptibilities were in good agreement with the model calculations.

More recently, we measured the superconducting transition of a sintered Y-Ba-Cu-O superconductor with Fe impurities in terms of harmonic ac susceptibilities.[15] Analyses of the results were made in the framework of the Kim-Anderson model with B_0, where $B(H)$ equations presented in this work were used. We found that the Kim-Anderson model with B_0 values in the vicinity of a few mT reproduces the data well.

ACKNOWLEDGMENTS

We are grateful to Dr. R. B. Goldfarb of the National Institute of Standards and Technology for valuable discussion and suggestions. The authors also express their thanks to Professor T. Takada and Professor Y. Bando of Kyoto University for stimulating discussion.

[1] C. P. Bean, Phys. Rev. Lett. **8**, 250 (1962).
[2] C. P. Bean, Rev. Mod. Phys. **36**, 31 (1964).
[3] H. London, Phys. Lett. **6**, 162 (1963).
[4] Y. B. Kim, C. F. Hempstead, and A. R. Strnad, Phys. Rev. Lett. **9**, 306 (1962).
[5] Y. B. Kim, C. F. Hempstead, and A. R. Strnad, Phys. Rev. **129**, 528 (1963).
[6] P. W. Anderson, Phys. Rev. Lett. **9**, 309 (1962).
[7] D.-X. Chen and R. B. Goldfarb, J. Appl. Phys. **66**, 2489 (1989).
[8] J. H. Watson, J. Appl. Phys. **39**, 3406 (1968).
[9] F. Irie and K. Yamafuji, J. Phys. Soc. Jpn. **23**, 255 (1967).
[10] I. M. Green and P. Hlawiczka, Proc. IEEE **114**, 1329 (1967).
[11] L. Ji, R. H. Sohn, G. C. Spalding, C. J. Lobb, and M. Tinkham, Phys. Rev. B **40**, 10 936 (1989).
[12] K.-H. Müller, Physica C **159**, 717 (1989).
[13] R. B. Goldfarb, A. F. Clark, A. I. Braginski, and A. J. Panson, Cryogenics **27**, 475 (1987).
[14] T. Ishida and R. B. Goldfarb, Phys. Rev. B **41**, 8937 (1990).
[15] K. Yamamoto, H. Mazaki, H. Yasuoka, S. Katsuyama, and K. Kosuge, Phys. Rev. B **46**, 1122 (1992).